

Simulation of reflectometry density changes using a 2D full-wave code

F. da Silva, M. Manso, and A. Silva

Citation: *Rev. Sci. Instrum.* **72**, 311 (2001); doi: 10.1063/1.1308997

View online: <http://dx.doi.org/10.1063/1.1308997>

View Table of Contents: <http://rsi.aip.org/resource/1/RSINAK/v72/i1>

Published by the [American Institute of Physics](#).

Related Articles

Modification of the collective Thomson scattering radiometer in the search for parametric decay on TEXTOR
Rev. Sci. Instrum. **83**, 113508 (2012)

Oblique electron-cyclotron-emission radial and phase detector of rotating magnetic islands applied to alignment and modulation of electron-cyclotron-current-drive for neoclassical tearing mode stabilization
Rev. Sci. Instrum. **83**, 103507 (2012)

0.22 THz wideband sheet electron beam traveling wave tube amplifier: Cold test measurements and beam wave interaction analysis
Phys. Plasmas **19**, 093110 (2012)

Measurements of parallel electron velocity distributions using whistler wave absorption
Rev. Sci. Instrum. **83**, 083503 (2012)

HELIOS: A helium line-ratio spectral-monitoring diagnostic used to generate high resolution profiles near the ion cyclotron resonant heating antenna on TEXTOR
Rev. Sci. Instrum. **83**, 10D722 (2012)

Additional information on *Rev. Sci. Instrum.*


Journal Homepage: <http://rsi.aip.org>

Journal Information: http://rsi.aip.org/about/about_the_journal


Top downloads: http://rsi.aip.org/features/most_downloaded

Information for Authors: <http://rsi.aip.org/authors>

ADVERTISEMENT



Does your research require low temperatures? Contact Janis today.
Our engineers will assist you in choosing the best system for your application.



10 mK to 800 K
Cryocoolers
Dilution Refrigerator Systems
Micro-manipulated Probe Stations

LHe/LN₂ Cryostats
Magnet Systems

sales@janis.com www.janis.com
Click to view our product web page.

Simulation of reflectometry density changes using a 2D full-wave code

F. da Silva,^{a)} M. Manso, A. Silva, and ASDEX Upgrade Team

Associação EURATOM/IST–Centro de Fusão Nuclear, Instituto Superior Técnico, 1046-001 Lisboa, Portugal

(Presented on 19 June 2000)

Broadband reflectometry is used to obtain density profiles in fusion plasmas using waves reflected at different plasma layers. The reflected signal can be severely affected by plasma fluctuations and/or fast density changes. In order to understand the plasma response, a finite difference time domain two-dimensional full wave code was developed. The code was used to study typical situations of fusion plasmas where important profile movements occur: when a rotating magnetic island is present and during an ELM. The numerical results are in good agreement with experimental results obtained in ASDEX and ASDEX Upgrade in the situations above. Our study demonstrates that contributions from the plasma movements are important and should be taken into account to obtain accurate profile measurements. © 2001 American Institute of Physics.

[DOI: 10.1063/1.1308997]

I. INTRODUCTION

Frequency modulated continuous wave (FM-cw) reflectometry measures the phase difference between a wave launched through the plasma (where it propagates and reflects at a cutoff layer) and a reference sample of the launched wave. In broadband swept reflectometry the frequency of the launched waves is swept over a broad frequency range to probe large regions of the plasma. It is usually assumed that the phase variation is mainly due to the distance to the several cutoff layers as follows: $\varphi[f(t)] = 4\pi f(t)/c \int_{x_0}^{x_c(f)} \mu[x, f(t)] dx - \pi/2$. From $\partial\varphi/\partial f$, the position of the plasma reflecting layers is obtained. Reflectometry results obtained in ASDEX Upgrade suggest that not only turbulence but also local and fast plasma movements can disturb the profile measurements, superimposing on the information of distance a contribution due to movement of the plasma layers. A finite difference time domain (FDTD) two-dimensional (2D) full wave code is used to study the impact of local plasma movement, such as those due to an electromagnetic localized mode (ELM) or a rotating magnetic island, on evaluated profiles. The code takes into account the specific detection and data analysis used in the ASDEX Upgrade diagnostic. The remainder of this article is organized as follows: in Sec. II the 2D code used is described. The numerical results and its comparison with experimental results are presented in Sec. III. Finally, in Sec. IV some conclusions are drawn about the importance of movement on the accuracy of reflectometry profiles.

II. CODE DESCRIPTION

The 2D code is used to obtain a two-dimensional solution for Maxwell curl equations for ordinary mode propagation in a cold plasma in the x – y plane with no gradients in the z axis. The plasma static magnetic field is assumed in the

z direction restricting the current flow to this same direction.¹ Plasma effects have been included in the response of the current density to the electric field.² With these simplifications, we obtain the following FDTD scheme:³

$$\begin{aligned}\mu_0 \epsilon_0 (\partial_t E_z)_{i+1/2, j+1/2}^n &= (\partial_x B_y - \partial_y B_x - \mu_0 J_z)_{i+1/2, j+1/2}^n, \\ (\partial_t B_x)_{i+1/2, j}^{n+1/2} &= -(\partial_y E_z)_{i+1/2, j}^{n+1/2}, \\ (\partial_t B_y)_{i, j+1/2}^{n+1/2} &= -(\partial_x E_z)_{i, j+1/2}^{n+1/2}, \\ (\partial_t J_z)_{i+1/2, j+1/2}^{n+1/2} &= (\epsilon_0 \omega_p^2 E_z)_{i+1/2, j+1/2}^{n+1/2}.\end{aligned}\quad (1)$$

To ensure the stability of the scheme, the Courant–Friedrichs–Lewy conditions, $\delta x, \delta y \geq 2c \delta t$, must be met, where $\delta x, \delta y$, and δt , are the spatial and the temporal increments, respectively. In this work we consider $\delta x = \delta y = \lambda_M/10$ and $\delta t = \tau_M/20$, where λ_M is the vacuum wavelength and τ_M the period for the maximum sweep frequency f_M . Equations (1) are solved on a computational grid where radiative boundary conditions (absorbing boundary conditions) have been imposed to prevent waves from reflecting at the boundary of the grid, forming a standing wave pattern that would completely obscure the results. The method proposed by Higdon⁴ was applied. For modeling the plasma the approach followed by Irby *et al.*¹ was adopted:

$$\frac{\omega_{p0}^2}{\omega^2} = \beta \exp(-\kappa\psi), \quad (2)$$

where $\psi = (x - x_0)^2/\omega^2 + (y - y_0)^2/(k\omega)^2$ defines curves of isodensity centered at (x_0, y_0) with elongation k along the y axis. In this work a single antenna, both for emission and reception, is used, reproducing the one-antenna configuration employed at the ASDEX Upgrade reflectometry diagnostic. Both the feeding–receiving waveguide and the antenna are modeled, imposing $E_z = 0$. A frequency modulated signal is “injected” into the system at the middle of the waveguide at instantaneous frequency⁵ $f(t) = f_c + f_\Delta x(t)$, with $f_\Delta < f_c$, where f_Δ is the frequency deviation, f_c the carrier frequency, and $x(t)$ the modulating signal, in our case a ramp. The instantaneous frequency of the signal varies from a minimum

^{a)}Electronic mail: tanatos@cfn.ist.utl.pt

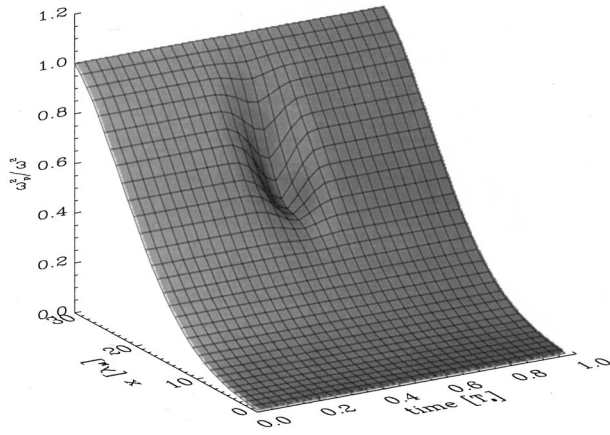


FIG. 1. Temporal evolution of ω_p^2/ω^2 along (x, y_0) for the simulated rotating plateau.

frequency $f_m = f_c$ to a maximum frequency $f_M = f_c + f_\Delta$ during the interval of a sweep T_s . The input FM signal is

$$E_{z_i}(t) = A_i \cos \left[\omega_c t + 2\pi f_\Delta \int_0^t x(\lambda) d\lambda \right]. \quad (3)$$

The output signal $E_{z_{\text{ant}}}(t)$ is monitored at the same point and results from the interference between the incident and the plasma reflected waves. $E_{z_{\text{ant}}}(t) = A(t) \cos[\omega(t)t + \varphi(t)]$ where $\varphi(t)$ is the phase difference between the reflected signal and the input signal. In order to reproduce the experimental conditions at the ASDEX Upgrade reflectometry system, namely, at detection (homodyne in the lower band channels and single-ended heterodyne in the higher channels), the $E_{z_{\text{ant}}}(t)$ signal is multiplied with a reference sample of the input signal $E_{\text{ref}}(t)$ and the low-frequency component is obtained by low pass filtering. The result is a reflectometry signal sensitive to the phase, such as measured in the experiment,

$$s(t) = S(t) \cos[\varphi(t)], \quad (4)$$

which is processed with the same tools used in experimental data.⁶

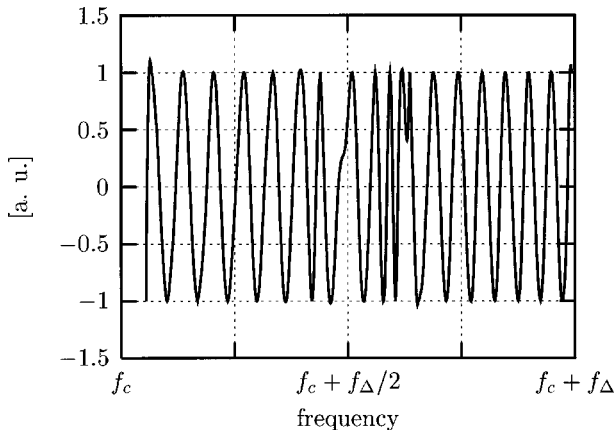


FIG. 2. Signal $s(t)$ for the simulated rotating plateau (one pass in front of the antenna).

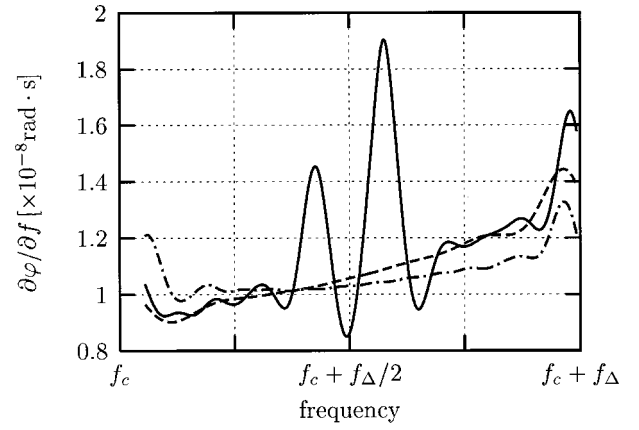


FIG. 3. Phase derivative ($\partial\varphi/\partial f$) for the simulated rotating plateau (one pass in front of the antenna). Lines (—) and (---) represent the derivatives for the unperturbed profile and for the profile with the maximum perturbation, respectively.

III. NUMERICAL SIMULATIONS

The density profile movements were simulated by disturbing the static behavior of the plasma, ω_p^2/ω^2 given by Eq. (2), with a perturbation function $p(t)$:

$$\frac{\omega_p^2}{\omega^2} = \frac{\omega_{p0}^2}{\omega^2} [1 + p(x, y, t)]. \quad (5)$$

Two types of situations were simulated: a time evolving plateau in the density profile like that produced by a rotating magnetic island⁷ and modification of the edge profile such as that observed during the occurrence of an ELM.⁸

A. Rotating density plateau

The rotating density plateau is simulated with the following perturbation:

$$p(x, y, t) = a \exp \left\{ -\frac{[x - x_p(t)]^2}{w_p^2} - \frac{[y - y_p(t)]^2}{(kw_p)^2} \right\}. \quad (6)$$

The center of the perturbation $[x_p(t), y_p(t)]$ gyrates along an isodensity line ψ_p according to the parametric equations $(x_0 + w_p \psi_p \cos[\theta(t)], y_0 + w_p k \psi_p \sin[\theta(t)])$ with $\theta(t) = \theta_0 + \omega_p t$, where θ_0 is the initial angular position of the plateau and ω_p the angular frequency of gyration of the perturbation

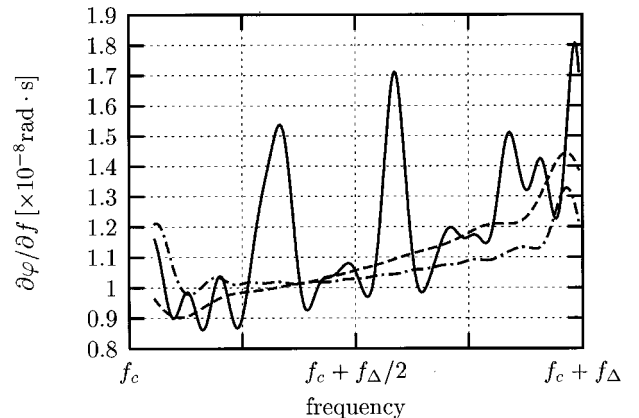


FIG. 4. Phase derivative $\partial\varphi/\partial f$ for the simulated rotating plateau (three passes in front of the antenna).

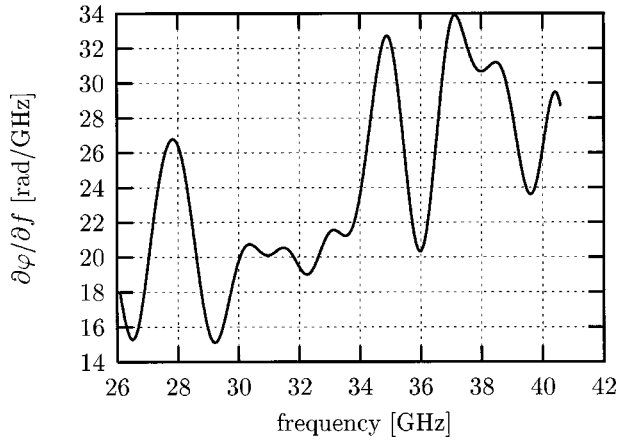


FIG. 5. Phase derivative for sweep 13 from ASDEX shot No. 29285 showing the effect of a rotating island.

along ψ_p . For a gyration period of $T_p = 5\pi/4T_s$ and an initial position $\theta_0 = (\pi + 2)/2$ the plateau appears once during a sweep in front of the antenna (see Fig. 1), perturbing the reflectometer signal as shown in Fig. 2. The corresponding phase derivative is displayed in Fig. 3. The evolution of $\partial\phi/\partial f$ deviates from those due to the two extreme static density profiles, (---) for the unperturbed profile and (-·-·-) for the profile with the maximum plateau. For a higher gyration period, $T_p = \pi/12T_s$, the plateau passes three times in front of the antenna during a sweep, “printing” several marks on the phase derivative (Fig. 4). In the old ASDEX tokamak, in low density plasmas and lower hybrid regimes very clear pictures of the effect of rotating magnetic islands were obtained due to the low level of plasma turbulence and large amplitude of the islands. Such an example is presented in Fig. 5 where the phase derivative for ASDEX shot No. 29285 (sweep 13) is depicted. The influence of a rotating island is seen well from a comparison of the nonperturbed plasma obtained before the magnetic mode was destabilized. A previous study⁷ showed that the period of the observed phase derivative perturbation is well correlated with the period of the rotation of the density plateau within the time frame of the frequency sweeping. From the study presented in Sec. III A it can be concluded that the numerical

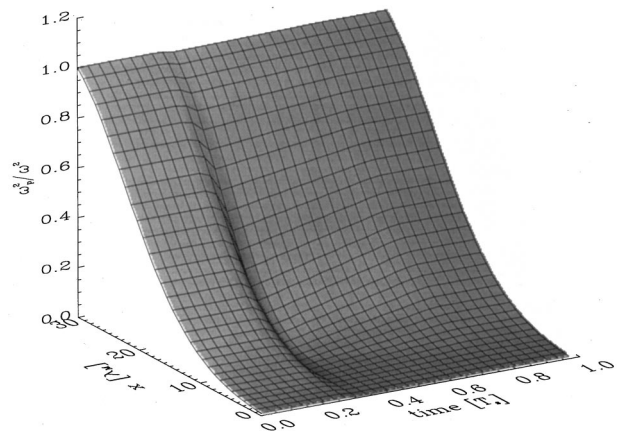


FIG. 6. Temporal evolution of ω_p^2/ω^2 along (x, y_0) for simulated edge movement.

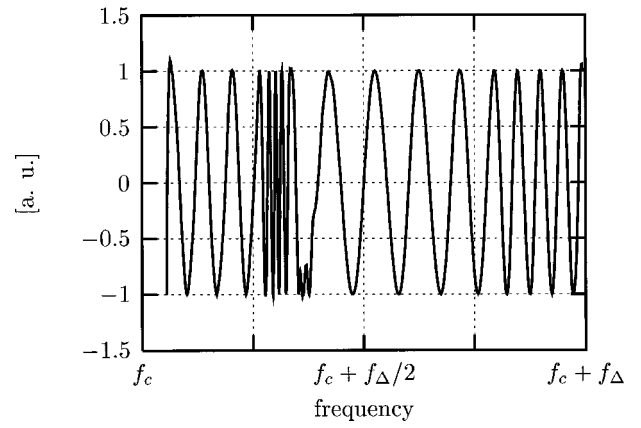


FIG. 7. Reflectometric signal $s(t)$ for simulated edge movement.

simulation using the 2D code, Sec. III A, reproduces quite well the oscillating pattern of the rotating density plateau.

B. Edge profile changes

To simulate the effect of an EML, where significant profile variations may occur during the sweeping time, the density profile is assumed to collapse on a fast time scale t_c and recover the initial profile characteristic of an H-mode plasmas on a longer time scale t_r , ($t_r/t_c = 9$), following the typical evolution of the density profiles measured in ASDEX Upgrade and in agreement with the temporal variation of the H_α signal. The perturbation of the edge is

$$p(x, t) = -a(t) \exp\left(-\frac{(x - x_p)^2}{w_p^2}\right), \quad (7)$$

where $a(t)$ varies from 0 to a maximum value a_M during t_c and back to zero during t_r . The edge movement occurs during the sweeping time T_s . The temporal evolution of the density profile at (x, y_0) can be seen in Fig. 6. The movement inwards, starting at $t = 1/4T_s$, reaches its maximum deviation at $t = 3/10T_s$ and then relaxes, recovering its original position at $t = 3/4T_s$. The reflectometer signal obtained in the above situation is presented in Fig. 7. For $f_c + 1/4f_\Delta \leq f \leq f_c + 3/10f_\Delta$ ($T_s/4 \leq t \leq 3T_s/10$) there is an abrupt increase of the beat frequency due to the effect of inward edge move-

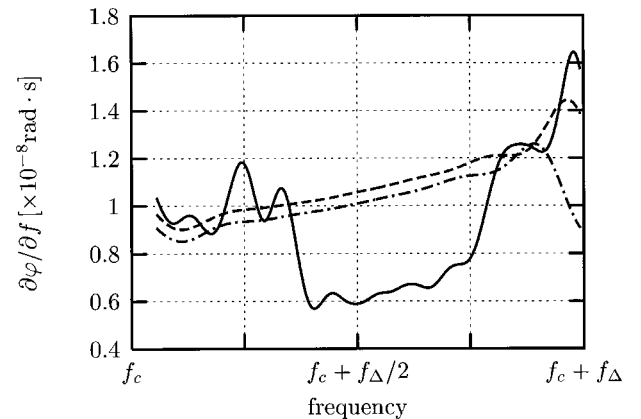


FIG. 8. Phase derivatives $\partial\phi/\partial f$ for simulated edge movement. Lines (---) and (-·-·-) represent the derivatives for the peaked and the flat profiles, respectively.

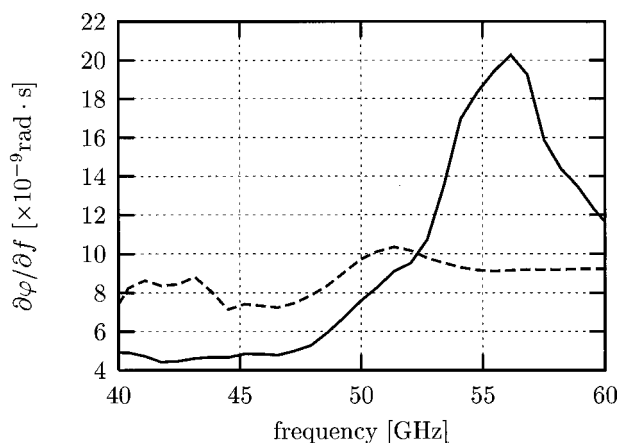


FIG. 9. Phase derivatives for sweeps 182 (—) and 239 (---), high field side, from ASDEX Upgrade shot No. 13224 obtained during an ELM.

ment. During the relaxation period of the density profile, $f_c + 3/10f_{\Delta} \leq f \leq f_c + 3/4f_{\Delta}$ ($3T_s/10 \leq t \leq 3T_s/4$), the beat frequency decreases, following outward movement of the plasma layers. The corresponding $\partial\phi/\partial f$ is represented in Fig. 8. The evolution of $\partial\phi/\partial f$ deviates from those due to the two extreme static density profiles, (---) for the peaked profile and (-·-·-) for the flat profile. This is due to two types of effects: one is the probing of different profiles along the sweep; the other is the appearance of Doppler terms associated with the velocity of profile changes.

In Fig. 9 is the phase derivatives obtained in ASDEX Upgrade during an EMLy H phase of shot No. 13224, corresponding to sweeps 182 and 239. Sweep 182 refers to the peak of the ELM (flat profile) and sweep 239 occurs after the ELM (peaked profile). As is observed, phase perturbations are present when profiles changes are occurring and disappear when the profile is quiescent, showing that the perturbation patterns are in agreement with the numerical results and may be attributed, at least partially, to plasma movement.

IV. DISCUSSION

The results obtained with the 2D code show that plasma movement causes important phase perturbations that should be considered in the analysis of density profile measurements with reflectometry. These deviations from the phase derivative curve of the unperturbed plasma profile include two types of contributions: one from variations of the position of the reflecting layers due to plasma movement, and the other due to the Doppler effects associated with the velocity of the profile changes. Our investigation will be pursued to determine the relative importance of the two contributions. Our study demonstrates that phase derivative perturbations must be understood in order to correctly evaluate the density profiles from reflectometry when plasma movement is important.

ACKNOWLEDGMENTS

Thanks are due to Dr. E. Holzhauser and to the authors' colleagues P. Varela and J. Santos for fruitful discussions. This work was carried out within the framework of the Contract of Association between the European Atomic Energy Community and Instituto Superior Técnico. Financial support from Fundação para a Ciência e Tecnologia and Praxis XXI was also received.

¹J. H. Irby, S. Horne, I. H. Hutchinson, and P. C. Stek, *Plasma Phys. Controlled Fusion* **35**, 601 (1993).

²I. H. Hutchinson, *Principles of Plasma Diagnostics* (Cambridge University Press, Cambridge, 1997).

³J. G. Blaschak and G. A. Kriegsmann, *J. Comput. Phys.* **77**, 109 (1988).

⁴R. L. Higdon, *Math. Comput.* **47**, 437 (1986).

⁵A. B. Carlson, *Communication Systems, Electrical and Electronic Engineering Series*, 3rd ed. (McGraw-Hill, New York, 1987).

⁶P. Varela, M. Manso, I. Nunes, J. Santos, F. Nunes, A. Silva, and F. Silva, *Rev. Sci. Instrum.* **70**, 1060 (1999).

⁷M. Manso, F. Serra, A. Silva, Y. Gatiás, F. Söldner, F. Wagner, and H. Zohm, Technical report, Associação EURATOM/IST (unpublished).

⁸P. Varela, M. Manso, S. Vergamiota, V. Grossmann, and Y. Santos, *Rev. Sci. Instrum.*, these proceedings.